17

High-Frequency Low Amplitude Atomic Force Microscopy

Hideki Kawakatsu,[1] Shuhei Nishida, Dai Kobayashi, Kazuhisa Nakagawa, and Shigeki Kawai[2]

[1] Institute of Industrial Science, the University of Tokyo, 4-6-1 Komaba, Meguro-ku, Tokyo 153-8505, Japan kawakatu@iis.u-tokyo.ac.jp
[2] Institute for Physics, University of Basel, 82 Klingelbergstrasse, Basel, Switzerland shigeki.kawai@unibas.ch

Abstract. This chapter explains a series of work carried out to implement atomic force microscopy (AFM) capable of operating at frequencies above 1–200 MHz with an amplitude of drive of a few 10–100 pm, both in the deflection and torsional modes. To implement such a microscope, various elements that constitute the AFM were reconsidered from scratch. The issues are; (i) Cantilever, (ii) Cantilever vibration excitation, (iii) Cantilever vibration detection, (iv) AFM head, and (v) Control scheme. The instrumental aspect of the microscope will be discussed in the former half, and the results obtained will be discussed in the latter.

17.1 Cantilever

Miniaturization of the cantilever enables increase of natural frequency f_o while maintaining a set value for the spring constant. Mass sensitivity of a cantilever improves with increasing frequency. For example, a cantilever with a natural frequency of 100 MHz, Q factor 10,000, spring constant 1 N/m, temperature 10 K, driven with an amplitude of drive of 10 nm has in principle, frequency noise comparable to change in mass by one hydrogen atom [1]. The use of small cantilevers is expected to introduce the function of mass detection at the molecular or atomic level to cantilever based microscopy. It should, however, be noted that exploiting the intrinsically high sensitivity of a nanocantilever, or coupling to a nano device is in itself a challenging topic, and has a lot of technical issues such as measurement related frequency noise to be cleared. Various attempts to fabricate small cantilevers or high-frequency cantilevers and beams have been made over the past 20 years. The term "nanocantilever" first appeared for a metallic ball held by a filiform neck. Formation of such a structure was predicted by Mullins in 1965, and confirmed experimentally in 1969 in the process of sharpening metal tips for field emission [2]. In the

S. Morita et al. (eds.), *Noncontact Atomic Force Microscopy*, NanoScience and Technology,
DOI: 10.1007/978-3-642-01495-6_17,

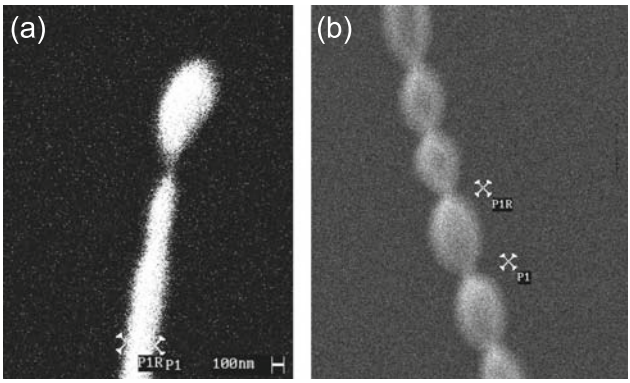

Fig. 17.1. Examples of metal nanocantilevers fabricated by heating a low tapered metal tip. (a) a 200 nm diameter metal ball ripening, (b) multiple ripening connected by filiform necks

early 1990s, N. Garcia and Vu Thien Binh published a paper on using such structures, which may attain a natural frequency of 1 GHz, as a force and mass sensor in AFM [3]. From 1995, the authors carried out a series of experiments on the method introduced earlier. Examples are shown in Fig. 17.1. In many cases, the tip-apex formed a sphere and a filiform neck due to Oswald ripening, but the morphological evolution was difficult to predict or control as shown in Fig. 17.1(b), not to mention batch fabricating a large number of cantilevers as a stock for AFM use [4]. Fabrication of AFM tips on the spherical mass was also an unsolved problem.

nanocantilever fabrication shifted to the use of MEMS fabrication techniques, where the cantilever could be tailor made with large numbers of hundreds or millions [5]. Due to the small size of the cantilever, the use of anisotropic etching of silicon was employed to ensure repeatability of fabrication that is not so much affected by the accuracy of the photolithography process [1]. Figure 17.2 shows some examples of the fabricated cantilevers. Some measure a few microns, and their natural frequency can be as high as 100 MHz. Attaining an amplitude of drive of around 100 pm, became the key issue in actually utilizing these cantilevers for AFM imaging. Fabrication of small cantilevers can be found in the literature [6–9].

17.2 Cantilever Vibration Excitation

The stable fabrication of small- and high-frequency cantilevers necessitated the selection of a reliable vibration excitation method. Massive piezo elements, a widely used device, attached to the base of the cantilever did not show a flat frequency response, and were not suitable for frequencies above

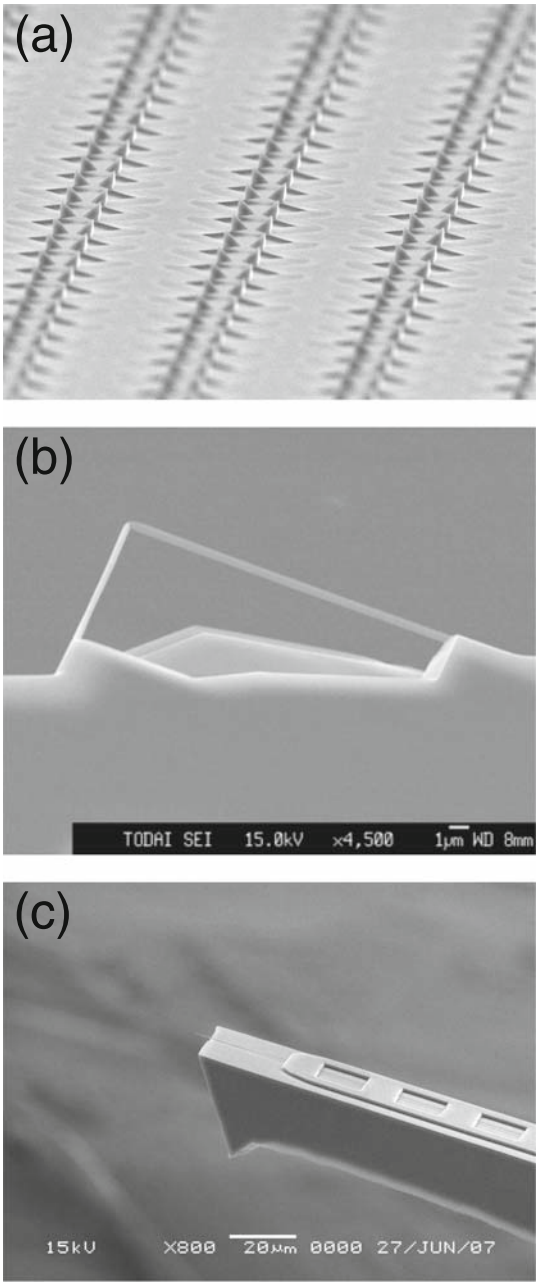

Fig. 17.2. Small cantilevers and oscillators fabricated from bulk silicon. (a) millions of cantilevers made by anisotropic etching of silicon, (b) triangular cantilevers composed of silicon nanowires, and (c) silicon nanowire cantilever with tip

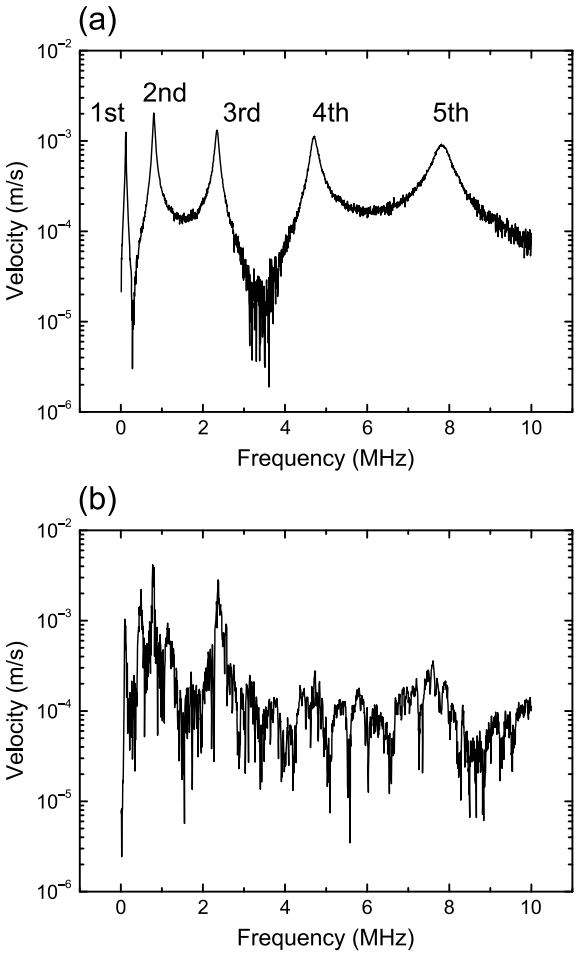

Fig. 17.3. Comparison of photothermal excitation and piezo excitation

ca. 5 MHz. Photothermal excitation proved to be effective in a wide range of frequency from DC to above 100 MHz [10–12]. In this method, a focalized beam from an intensity modulated laser diode was guided to the surface of the cantilever through an objective lens. For commercially available cantilevers, an intensity of 1 mW was sufficient in vacuum, and 2 mW in water. Figure 17.3 shows a comparison of photothermal excitation and piezo excitation made with the same liquid AFM. Since the actuation acts on the oscillator directly, various vibration modes of the oscillator could be excited with clarity. Phase rotation around resonance was also clear, facilitating phase based controls. Positioning of the excitation laser spot enabled the selection of modes to be excited, while surpressing unexpected mode-hopping. Other possible excitation methods have been employed in the field of mass sensing

with mechanical oscillators, such as, electrostatic excitation, joule heating excitation [13], surface acoustic wave excitation, magnetic excitation [14], and piezoelectric actuation [15, 16]. In terms of simplicity, photothermal excitation is favorable, but for cantilevers measuring below 1 μm in width or length, the other methods listed earlier may prove to be more feasible.

17.3 Cantilever Vibration Detection

Stable fabrication of micron sized cantilevers also facilitated the comparison and development of various cantilever vibration detection schemes. Issues put to question were (i) focalization down to the diffraction limit to accommodate micron sized cantilevers, (ii) capacity to measure the vibration of cantilevers up to the 100 MHz regime, (iii) ease of use in UHV and cryostats, (iv) compatibility with the photothermal excitation method, and (v) stability. Optical methods were considered first to lessen the requirements on the cantilever. Two methods were considered; (i) Homodyne detection using a focusing mirror and a reference arm incorporated with in the millimeter sized optical probe, with two optical fibres supplying and retrieving light to and from the optical probe and (ii) heterodyne laser Doppler detection with various carrier generating schemes. Among the two, the latter was superior in performance due to the high signal-to-noise ratio and stable operating point, typical of heterodyning techniques. The fact that velocity was directly measured acted favourably for small- and high- frequency cantilevers because the velocity signal increased in proportion to frequency for a given amplitude of drive. As the result, the noise floor of the measurement scheme gave a $1/f$ decrease in

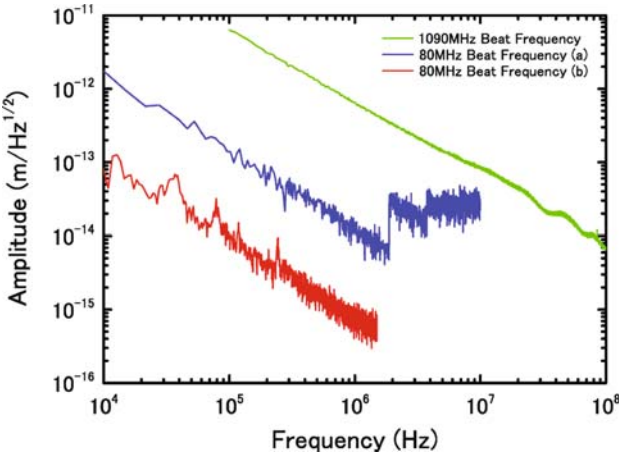

Fig. 17.4. Typical noise floors of the heterodyne laser Doppler interferometer with 80 MHz or 1.1 GHz carrier

terms of displacement [17]. Figure 17.4 shows typical noise floors for various sensitivity and frequency ranges of the Doppler interferometer. Noise level below 1 fm/$\sqrt{}$Hz was attained around 2 MHz. For high-frequency measurement above 20–200 MHz, the beat between two longitudinal modes of a He–Ne laser at 880 MHz plus a 200 MHz AOM, or a cascade of two AOMs operating at 540 MHz were used to generate a carrier above 1 GHz. For frequency range below 20 MHz, the use of a 80 MHz AOM proved to give the best performance in terms of signal-to-noise ratio, and are used our liquid AFMs and UHV AFMs operating below 20 MHz. The method could detect the vibration of a tungsten suboxide whisker measuring 70 nm in diameter, but requiring a narrow bandwidth in such a case, and not suitable as yet to accommodate such cantilevers for AFM and image with a reasonable scan rate. On the other hand, cantilevers measuring a few microns, and larger than the focal diameter could be measured with a good signal level up to 200 MHz. Heterodyne detection was effective in avoiding cross-talk between optical vibration excitation and measurement down to the fm level, since measurement was carried out around 80 MHz or 1.1 GHz, and not in the vicinity of the cantilever vibration modes.

17.4 AFM Head

Since detection and excitation of the cantilever vibration can be implemented by optical means, the design of the AFM is a relatively simple matter of positioning a focusing lens with respect to the cantilever. Figure 17.5 depicts the schematic of the laser Doppler optics with a 80 MHz AOM, and Figure 17.6 depicts a liquid AFM composed of an inverted optical microscope objective, two photothermal excitation lasers operating at 405 and 780 nm, illumination laserdiode, a CCD and the laser Doppler optics. The returning beam of the laser Doppler measurement is collected through the same optical path, so steering of the laser beam with a mirror was enough to position the laser spot on the designated location of the cantilever. Figure 17.7 shows the optical probe of an UHV AFM. Four beams guided to the optical probe are, the measurement beam, the reference beam, the photothermal laser beam, and the illumination beam. Guiding the reference arm to the optical probe was effective in decreasing the effect of axial and orthogonal vibration of the optical probe with respect to the laser source and the axis of the laser beam. The same optics was also applied to an UHV TEMAFM, with the exception of the focusing lens, which was replaced by a grin lens measuring 2 mm in diameter. The lens was inserted between the yokes of the TEM. Equivalent signal-to-noise ratio was confirmed, but the excitation efficiency was lower due to achromatic error of the lens. An optical probe with the function of Doppler measurement only was also implemented, and in such a case, the optical probe was connected to a polarization maintaining optical fibre [17].

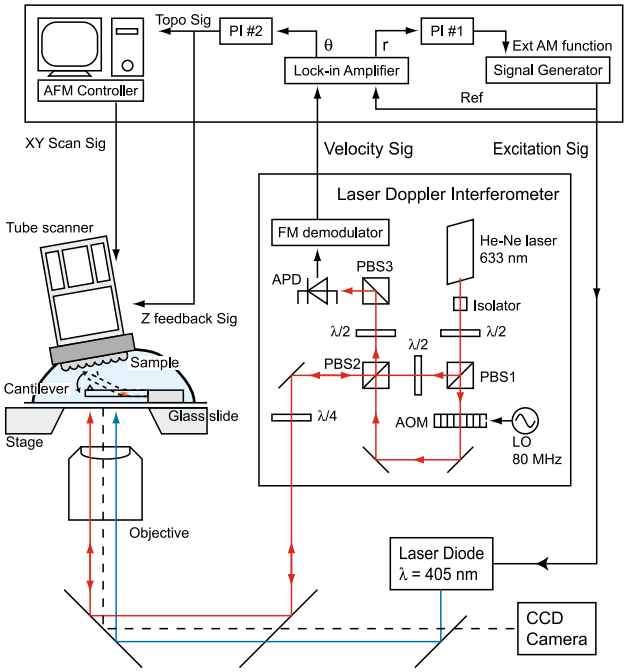

Fig. 17.5. Schematic of the liquid AFM with heterodyne laser doppler interferometry and photothermal vibration excitation. Self-excitation is not utilised in imaging

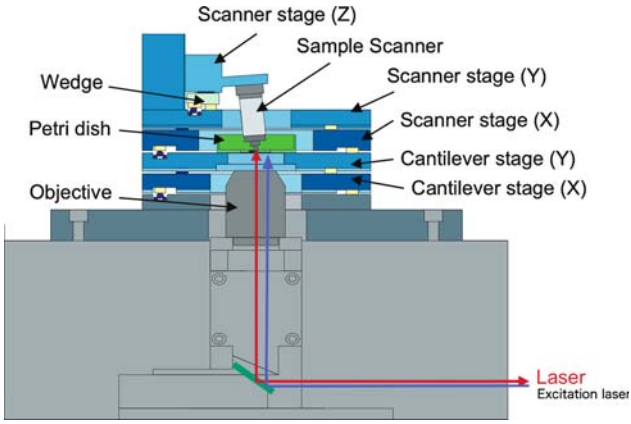

Fig. 17.6. Head of the liquid AFM

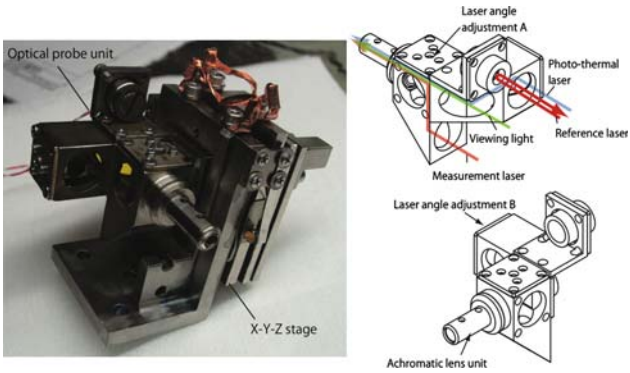

Fig. 17.7. Optical probes of UHV AFM. (a) for a Low temperature UHV AFM. For an UHV TEMAFM, a longer objective with a grin lens at the apex is inserted in the pole gap of the TEM

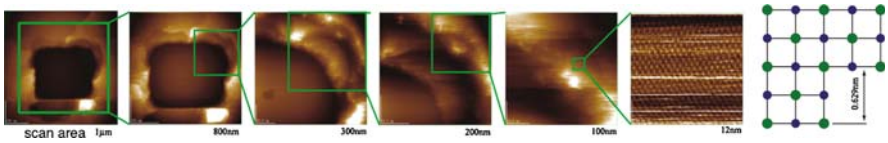

Fig. 17.8. KCl imaged from low resolution to high resolution. The imaged area is zoomed to a terrace at the top right corner

17.5 Control Scheme

For UHV AFM applications, the Doppler interferometer was inserted within the self-excitation loop of the cantilever, together with a phase shifter and auto gain control. The configuration is not so different from other UHV AFM, expect for the fact that the velocity signal is used for the self excitation. In the case of the liquid AFM, we have adopted a different scheme, as depicted in Fig. 17.5. The tip approach is accomplished by monitoring the self-excitation frequency of the cantilever, where an FM controlled signal generator is used within the self-excitation loop. After the cantilever has reached its operating point, in other words, the designated frequency shift has been met, the FM function of the signal generator is turned off, and the cantilever is driven at a fixed frequency. At the same time, tip to sample distance regulation is activated, in such a manner that the phase shift between the signal generator and the Doppler output is kept to a constant value by proportional-integral control. As the result, an equi-frequency shift surface can be mapped at the chosen value of the frequency shift. The advantage of this method over the conventional FM, AM, or PM methods is that: (i) the vibration amplitude is maintained in a damped environment, and imaging of stepped or corrugated surfaces is possible, (ii) the operating point can be reached in a gentle, quasi-static fashion, since approach is done in the slow self-excitation mode. Figure 17.8 shows KCl imaged in saturated butanol. Scanning with a relatively

high-positive frequency shift leads to dessorption of the KCl ions, leaving a square hole corresponding to the scanned area. Then imaging the same area can be carried out by lowering the amount of frequency shift. In the figure, the image area is zoomed to a small terrace on the top right corner of the hole, eventually attaining atomic resolution [18]. The result demonstrates the potential of the control method to image rough surfaces in liquid, and attain atomic resolution.

17.6 Imaging with Small Amplitude of Drive

As depicted in Fig. 17.4, the noise floor of the Doppler interferometer reaches the 1 fm/$\sqrt{}$Hz level around 1 MHz. This allows for a relatively large signal-to-noise margin, giving the possibility to either (i) scan very fast by using a wide bandwidth, or (ii) image with a very small amplitude of drive. We have demonstrated the latter, since imaging with small amplitude has such physical significance as (i) local three-dimensional probing of the field that allow linear modelling of the system, (ii) possibility to map sub Å feature, and (iii) less disturbing to the sample and the structured liquid molecules in liquid. Figure 17.9 shows a series of Si(111) 7×7 surfaces imaged with an amplitude of drive of less than 1 Å [19]. The image with the smallest amplitude of drive reaches a value below 0.3 Å, which is a factor of 1/1,000 smaller than the value used when true atomic resolution was first achieved ten years earlier. The cantilever used for the imaging was a commercially available cantilever with a natural frequency of about 300 kHz, and a spring constant of 40 N/m, but driven at the second mode of deflection at around 1 MHz.

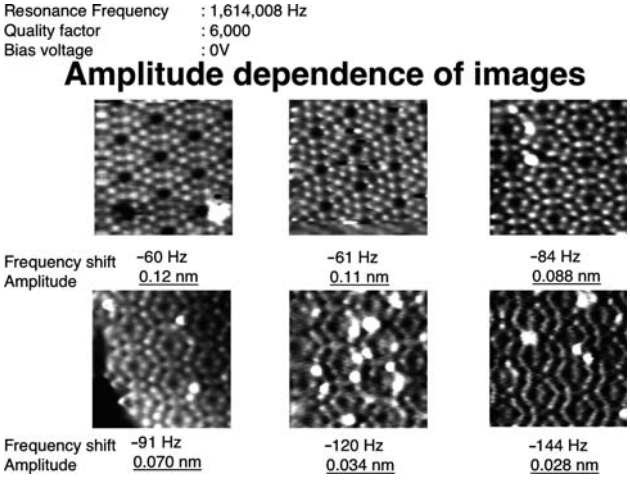

Fig. 17.9. Images of Si(111) 7×7 imaged with different amplitude of drive. The smallest amplitude can be as small as 10 pm

The higher spring constant of the higher mode is in part responsible for the success of imaging with the small amplitude of drive. Imaging of metastable surfaces of quenched Si(111), as well as single atom manipulation at room temperature were confirmed with the AFM operating with an amplitude of drive of around 100 pm or less [20, 21]. The same cantilever was driven at around 5 MHz, the third mode of deflection. Despite the increased level of spring constant, in the kN/m range, cleaved graphite, commonly known to be difficult to be observed by AFM due to its low level of force corrugation, was imaged readily [22]. Simultaneous imaging of STM and AFM gave new understanding of the contrast mechanism, the origin of giant corrugations, and contrast mechanism of AFM on graphite [23]. In liquid, true atomic resolution of such samples as NaCl, KCl, and mica were confirmed, also with sub Å amplitudes [24]. When imaging mica in pure water, lattice structures were seen to exist for a vertical approach of the tip to the sample for a range of over 10 Å, with a marked shift in vertical stiffness of the sample between the lattice layers. The fact that atomic resolution was obtained for a wide range of z position, is a strong indication that the AFM is mapping structured liquid molecules with unprecedented resolution. Fig.17.10 shows features obtained on mica immersed in pure water, which could be acquired with subangstrom amplitude of drive. High contrast features with a 60 pm height difference could be resolved [25].

17.7 Lateral Dynamic Force Microscopy

Various vibrational modes could be excited with a piezo element, or by the earlier mentioned photothermal excitation, with the latter capable of driving from DC to frequencies above 100 MHz. As depicted in Fig. 17.3, imaging with the torsion of the cantilever was just a matter of selecting the operating frequency to match the torsional mode of the AFM cantilever. In the case of photothermal excitation, the obtained vibration signal was even more clearer due to the low suprious vibrations. Figure 17.11 shows Si(111) 7×7 imaged with the first torsional mode of a commercially available cantilever. Although not the entire field of view, features corresponding to the 7×7 structure could be resolved. This was imaged with the FM mode, and no tunneling current was used for the control. A more detailed study was carried out using tunneling for gap control, and with an amplitude of drive of a few 10 to around 100 pm. Due to the drastically reduced level of lateral amplitude, lateral force gradient could clearly be resolved at the atomic level. Simulation based on first-principle calculation matched very well the experimental results, and also could explain the artefacts observed to be due to cross talk of vertical and lateral vibrations [26].

In the case of the liquid AFM operated in the torsional mode, clear true atomic resolution images could be resolved readily using the control scheme introduced in the former chapter. Fig. 17.12 shows mica imaged with the torsional mode at 1.16 MHz, amplitude to drive 130 pm. The image contrast

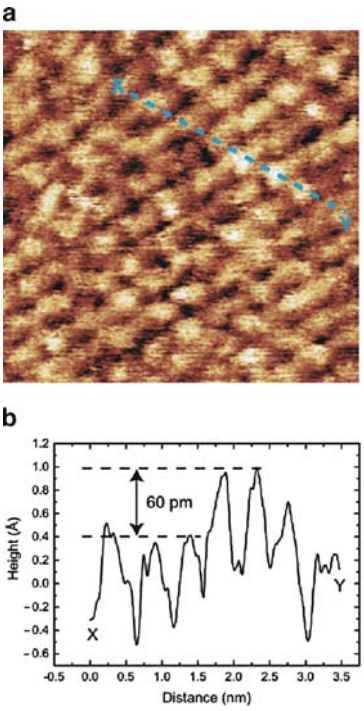

Fig. 17.10. Mica imaged in pure water. frequency: 964.750 kHz, amplitude: 99 pm

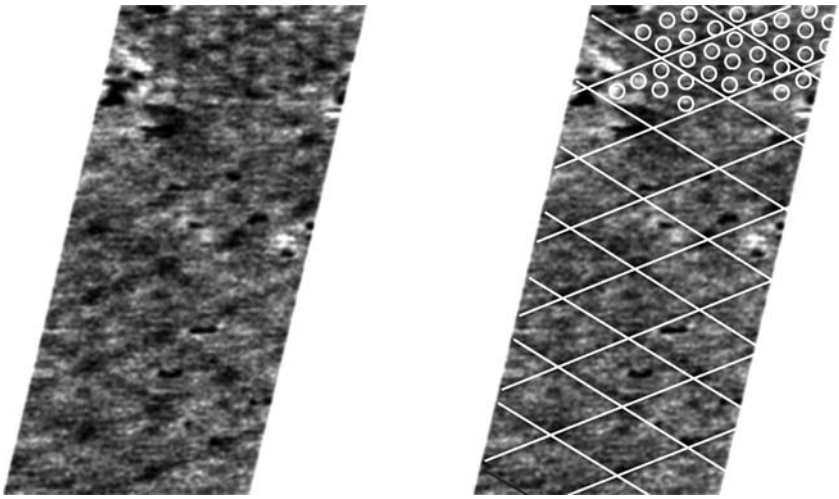

Fig. 17.11. Si(111) 7×7 imaged by dynamic mode lateral force microscopy. The tip height was regulated by the frequency shift of the torsional self excitation

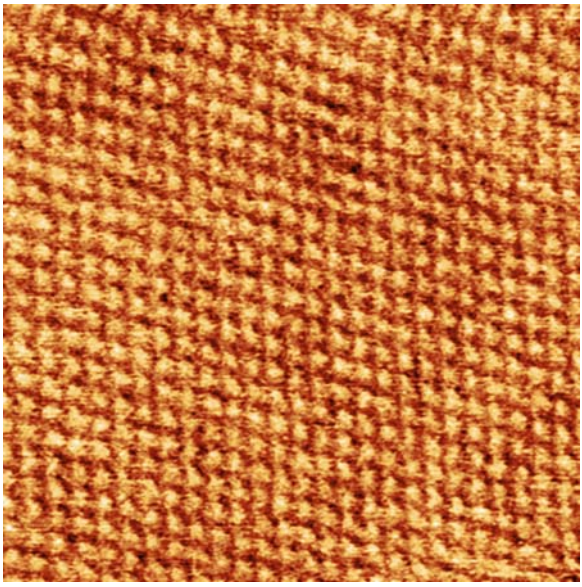

Fig. 17.12. Image of mica acquired with dynamic mode lateral force microscopy. Frequency 1.1 MHz, amplitude of drive 100 pm

was exceedingly better than lateral force imaging in vacuum [27]. In liquid AFM, the effect of amplitude and frequency of drive on the structured liquid molecules needs to be taken into account, since the choice these conditions may drastically change the physics of the confined region. At the expense of losing signal-to-noise ratio, it is meaningful in liquid AFM to decrease the amplitude of drive to the 10 pm order. It should also be pointed out that the surface mapped in liquid AFM may not be the true surface. The existence of a single molecule resting in registry with the lower layer is an indication that there are other similar molecules with a shorter lifetime equally resting on the surface. Due to the bandwidth of the detection or the electronic circuitry, the existence of the upper layer may have been overlooked and not mapped. Change of bandwidth at the cost of signal-to-noise ratio may reveal and possibly allow mapping of the upper layers. Temperature control in liquid AFM is underway to measure change in surface structure and to carry out time resolved measurements.

17.8 Summary

Small amplitude high-frequency AFM was discussed, with one eventual goal as the use of nanocantilevers as the force detector. Further miniaturization of the cantilever is faced with the issue of how to maintain a suitable level of

signal-to-noise ratio and bandwidth for their measurement. In other words, the issue comes down to how to couple to nanodevices with a reasonable bandwidth to exploit their intrinsically high sensitivity. This can be put in a perspective of how to concentrate energy used for measurement in a small volume. Exploring techniques both old and new, such as electron emission [28, 29] and near field optics is needed for a significant breakthrough.

References

1. H. Kawakatsu, S. Kawai, D. Saya, M. Nagashio, D. Kobayashi, H. Toshiyoshi, and H. Fujita, Rev. Sci. Instrum. **73**, 2317 (2002)
2. M. Drechsler, A. Piquet, R. Uzan, and Vu Thien Bihn, Surf. Sci. **14**, 457 (1969)
3. Vu. Thien Binh, N. Garcia, and A.L. Levanuyk, Surf. Sci. Lett. **301**, L224 (1994)
4. H. Kawakatsu, D. Saya, M. de Labachelerie, H.-J. Hug, and H.-J. Guentherodt, Jpn. J. Appl. Phys., Part 1 **38**, 3954 (1999)
5. H. Kawakatsu, H. Toshiyoshi, D. Saya, and H. Fujita, Jpn. J. Appl. Phys., Part 1 **38**, 3962 (1999)
6. J.L. Yang, M. Despont, U. Drechsler, B.W. Hoogenboom, M.E. Muller, P.L.T. M. Frederix, M.E. Muller, S. Martin, A. Engel, P. Vettiger, and H.J. Hug,. Appl. Phys. Lett. **86**, 134101 (2005)
7. S. Hosaka, K. Etoh, A. Kikukawa, and H. Koyanagi, J. Vac. Sci. Technol. B, **94**, 94 (2000)
8. J.L. Yang, T. Ono, and M. Esashi, Appl. Phys. Lett., **77**, 3860 (2000)
9. M.B. Viani, T.E. Schaffer, A. Chand, M. Rief, H.E. Gaub, and P.K. Hansma, J. Appl. Phys., **86**, 2258 (1999)
10. N. Umeda, S. Ishizaki, and H. Uwai, J. Vac. Sci. Technol. B **9**, 1318 (1991)
11. G.M. Kim, S. Kawai, M. Nagashio, H. Kawakatsu and J. Brugger, J. Vac. Sci. Technol. B **22**, 1658 (2004)
12. S. Nishida, D. Kobayashi, H. Kawakatsu, and Y. Nishimori, J. Vac. Sci. Technol. B 27, 964 (2009)
13. I. Bargatin, I. Kozinsky, and M.L. Roukes, Appl. Phys. Lett. **90**, 093116 (2007)
14. X.L. Feng, Rongrui He, Peidong Yang, and M.L. Roukes, Nano lett, **7**, 1953 (2007)
15. Sotiris C. Masmanidis, Rassul B. Karabalin, Iwijn De Vlaminck, Gustaaf Borghs, Mark R. Freeman, Michael L. Roukes, Science **317** no. 5839, 780 (2007)
16. J.L. Arlett, J.R. Maloney, B. Gudlewski, M. Muluneh, and M.L. Roukes, Nano Lett. **6**, 1000 (2006)
17. S. Kawai, D. kobayashi, S. Kitamura, S. Meguro, and H. Kawakatsu, Rev. Sci. Instrum. **76**, 083703 (2005)
18. S. Nishida, D. Kobayashi, T. Sakurada, T. Nakazawa, Y. Hoshi, and H. Kawakatsu, Rev. Sci. Instrum. 79, 123703 (2008)
19. S. Kawai, S. Kitamura, D. Kobayashi, S. Meguro, and H. Kawakatsu, Appl. Phys. Lett. **86**, 193107 (2005)
20. S. Kawai, F. Rose, T. Ishii, H. Kawakatsu, J. Appl. Phys. **99**, 104312 (2006)
21. S. Kawai, and H. Kawakatsu, Appl. Phys. Lett. **89**, 023113 (2006)

22. S. Kawai and H. Kawakatsu, App. Phys. Lett. **88**, 133103 (2006)
23. S. Kawai and H. Kawakatsu, Phys. Rev. B 79, 115440 (2009)
24. S. Nishida, D. Kobayashi, T. Sakurada and H. Kawakatsu unpublished
25. S. Nishida, D. Kobayashi, T. Sakurada, T. Nakawasa, Y. Hoshi, and H. Kawakatsu, Rev. Sci. Instrum. 79, 123703 (2008)
26. S. Kawai, N. Sasaki, and H. Kawakatsu, Phys. Rev. B 79, 195412 (2009)
27. S. Nishida, D. Kobayashi and H. Kawakatsu, unpublished
28. E. Mueller. Z. Phys. **102**, 734 (1936)
29. K. Jensen, Kwanpyo Kim and A. Zettl, Nature Nanotechnology **3**, 533 (2008)